

Morphing ab initio potentials: A systematic study of Ne–HF

Markus Meuwly and Jeremy M. Hutson

Citation: *The Journal of Chemical Physics* **110**, 8338 (1999); doi: 10.1063/1.478744

View online: <http://dx.doi.org/10.1063/1.478744>

View Table of Contents: <http://scitation.aip.org/content/aip/journal/jcp/110/17?ver=pdfcov>

Published by the [AIP Publishing](#)

Articles you may be interested in

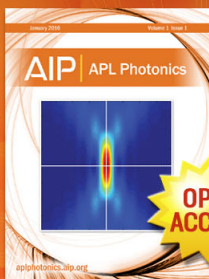
[A new ab initio intermolecular potential energy surface and predicted rotational spectra of the Ne–H₂S complex](#)
J. Chem. Phys. **136**, 214307 (2012); 10.1063/1.4725715

[Ab initio study of Rg–N₂ and Rg–C₂ van der Waals complexes \(Rg=He, Ne, Ar\)](#)
J. Chem. Phys. **119**, 909 (2003); 10.1063/1.1579464

[An ab initio study of the Ar–HCN complex](#)
J. Chem. Phys. **110**, 1416 (1999); 10.1063/1.478016

[An ab initio study of He–F₂, Ne–F₂, and Ar–F₂ van der Waals complexes](#)
J. Chem. Phys. **110**, 860 (1999); 10.1063/1.478053

[Polarizabilities of CO, N₂, HF, Ne, BH, and CH⁺ from ab initio calculations: Systematic studies of electron correlation, basis set errors, and vibrational contributions](#)
J. Chem. Phys. **109**, 4745 (1998); 10.1063/1.477086



Launching in 2016!
The future of applied photonics research is here

OPEN
ACCESS

AIP | APL
Photonics

Morphing *ab initio* potentials: A systematic study of Ne–HF

Markus Meuwly and Jeremy M. Hutson

Department of Chemistry, University of Durham, South Road, Durham DH1 3LE, England

(Received 28 October 1998; accepted 6 February 1999)

A procedure for “morphing” an *ab initio* potential energy surface to obtain agreement with experimental data is presented. The method involves scaling functions for both the energy and the intermolecular distance. In the present work, the scaling functions are parametrized and determined by least-squares fitting to the experimental data. The method is tested on the system Ne–HF, for which high-resolution infrared spectra are available. It is shown to work well even with relatively low-level *ab initio* calculations. Several basis sets are investigated at the CCSD(T) correlation level, including various aug-cc-*pVnZ* basis sets and the specially-tailored Ne–HF basis set of O’Neil *et al.* All give good results after morphing, but the changes needed to match experiment are much smaller for the O’Neil basis set. The use of MP2 calculations is also investigated: again, the MP2 potential is quite satisfactory after morphing, but requires much more modification than the CCSD(T) potential. © 1999 American Institute of Physics. [S0021-9606(99)31417-3]

I. INTRODUCTION

The last decade has seen enormous advances in our understanding of potential energy surfaces, especially in the field of intermolecular forces. For prototype systems such as Ar–HF,¹ Ar–HCl,² He–CO,³ Ar–CO₂,⁴ (HF)₂,⁵ and (HCl)₂,⁶ it has been possible to use extensive experimental information from the spectroscopy of Van der Waals complexes to develop accurate and reliable potential energy surfaces. In parallel with this, there have been substantial advances in electronic structure calculations: it is now possible to carry out *ab initio* calculations that give potentials approaching spectroscopic accuracy.

Although *ab initio* methods have advanced, the calculations needed to get high accuracy remain expensive and laborious. Large basis sets and high-level correlation treatments are essential, and very large numbers of points are needed to give an adequate coverage of configuration space, especially for molecule–molecule systems. It is unlikely that systematic errors due to basis set incompleteness and approximate correlation treatments will ever be eradicated completely. Under these circumstances, there is scope for even the best *ab initio* surface to be improved using experimental results from high-resolution spectroscopy or elsewhere.

One approach that has considerable appeal is to take a good *ab initio* potential and modify it slightly to fit the experimental data available. This may be done in various ways. If the potential can be decomposed into different physical contributions, its components may be modified individually to improve the fit to experimental data.^{3,4} However, the success of this approach depends on the availability of a suitable decomposition. An attractive alternative is to work with the interaction energy itself. Various workers^{7–9} have simply scaled *ab initio* potentials by a constant factor to improve the agreement with experiment. This approach modifies the energetics while leaving the geometries of stationary points unchanged. Conversely, Bowman *et al.*^{10–12} have morphed

ab initio potential surfaces for HCO and HCN by multiplying the coordinates by a scaling function before calling the potential routine, thus modifying the geometries of stationary points while leaving the energetics unchanged. They also introduced a subsequent energy scaling,¹¹ applied with the coordinate scaling held fixed. Our approach differs slightly, in that we introduce energy and coordinate scaling functions *simultaneously*, thus allowing for correlations between the two.

The objective of the morphing process is to achieve agreement with experimental data by making changes to the potential energy surface that are as small as possible. However, “as small as possible” is a term that has no absolute meaning. The scientist doing the fitting must make judgments about which features of the original potential should be preserved and which can be adjusted. For example, if the original surface has two minima at different geometries, it may well be possible to reproduce the experimental data either by holding one well depth fixed and varying the other, or by adjusting both well depths simultaneously. The choice is one that must be made using physical understanding and intuition, and the quality of the final surface may depend crucially on the choice that is made. We believe that such physical choices should be made as explicit as possible, not hidden under layers of mathematical formalism.

The optimization process is conceptually simple for a potential surface that is parametrized directly in terms of well depths and equilibrium distances. All that is necessary is to choose which parameters should be varied and then to carry out a least-squares fit to the experimental data to determine optimum values. However, this approach is not ideal for adjusting pointwise *ab initio* potentials, because a fitted functional form will not go through all the *ab initio* points in the first place. The flexibility of the final potential is thus limited by the choice of functional form. A more attractive approach is to start with a potential energy surface that interpolates between the *ab initio* points and is then “morphed” to bring it into agreement with experiment. Various

interpolation schemes could be used for this; in the present work, we use the reproducing kernel Hilbert space (RKHS) interpolation method,¹³ which provides an efficient approach that can readily be extended to many dimensions.

The present paper has three objectives. First, we describe an approach to potential morphing that provides an economical representation of the surface, yet lays the essential physical choices open to inspection. Second, we apply our method to the test case of Ne–HF, which has been studied before^{14,15} but for which no definitive intermolecular potential exists. Last, we investigate the robustness of the method by repeating the calculations using *ab initio* potentials of poorer quality, in order to establish the minimum level of calculation that can provide a useful basis for morphing. In the process, we reach some interesting conclusions about the quality of the unmodified potentials produced by different basis sets and correlation treatments.

II. PREVIOUS WORK ON NE–HF

High-resolution infrared spectra of Ne–HF were first reported by Nesbitt *et al.*,¹⁶ who observed and analyzed the HF stretching fundamental band ($\nu_{jKn})=(1000)\leftarrow(0000)$ and the Π bending combination band ($1110)\leftarrow(0000)$. The complex shows interesting dynamical features such as J -dependent predissociation rates, which allowed the determination of a rigorous upper limit to the binding energy. Microwave spectra of Ne–HF have also been observed.¹⁷

In subsequent studies, the spectroscopy of the deuterated counterpart Ne–DF was investigated.¹⁵ For Ne–DF, a richer spectroscopy was observed because of the smaller rotational constant of DF, which allows more bending excitation of the complex without predissociation. Lovejoy and Nesbitt¹⁵ observed the DF stretching fundamental ($1000)\leftarrow(0000)$ and combination bands involving the Van der Waals stretch, ($1001)\leftarrow(0000)$, the Π bend, ($1110)\leftarrow(0000)$, and the Σ bend, ($1100)\leftarrow(0000)$. (The Σ bend combination band is designated ($12^0_0)\leftarrow(00^0_0)$ by Lovejoy and Nesbitt, because the Σ bend correlates with $j=1$ for a free internal rotor but with the overtone of the bend for a near-rigid linear molecule.)

In parallel with the experimental efforts, O'Neil *et al.*¹⁴ constructed an *ab initio* potential energy surface using the correlated electron pair approximation (CEPA) and used it in rovibrational calculations. The agreement between the experimental results on Ne–HF and the theoretical predictions was reasonable. Lovejoy and Nesbitt¹⁵ subsequently adjusted the CEPA potential to reproduce their observed spectra for Ne–DF, and the resulting potential also gave a good account of the spectra of Ne–HF.

III. AB INITIO CALCULATIONS

The present work uses *ab initio* calculations to provide a starting point for morphing. For a system such as Ne–HF, a large part of the attraction arises from dispersion forces. The most important factors affecting the quality of the potential are thus the level of the correlation treatment used and the basis set employed.

There are many basis sets available, tailored for different applications. In recent work on intermolecular forces, the augmented correlation-consistent (aug-cc) basis sets of Dunning and co-workers^{18,19} have become popular. Although these basis sets are not specifically optimized for intermolecular interactions, they do provide economical representations of correlation effects. In addition, the basis sets exist at a variety of different levels: double-zeta (VDZ), triple-zeta (VTZ), quadruple-zeta (VQZ), etc., and thus allow a systematic investigation of the effect of increasing basis-set size.

On the other hand, specially designed basis sets exist for a handful of systems, including Ne–HF. In their original *ab initio* work on this system, O'Neil *et al.*¹⁴ put considerable effort into designing a basis set that gave a good account of the effects important in intermolecular forces.

We decided to work principally with the aug-cc- $pVnZ$ series of basis sets but to compare the results with those obtained with the basis set of O'Neil *et al.* O'Neil's basis set has highest angular momentum functions that parallel the aug-cc- $pVTZ$ basis set but has less highly contracted s and p functions.

Our initial concern was to compare the performance of the different basis sets using as complete a correlation treatment as possible. We therefore decided to work with coupled-cluster calculations at the CCSD(T) level of theory. The effect of using lower-level correlation treatments (CEPA and Møller–Plessett perturbation theory) will be considered later.

The present work uses a standard Jacobi coordinate system, in which r is the H–F distance, R is the distance from the HF center of mass to Ne, and θ is the angle measured at the center of mass (with $\theta=0$ corresponding to the linear Ne–H–F geometry). The grid on which energies were calculated is chosen to facilitate subsequent calculations of the bound states. In particular, the evaluation of the necessary integrals is stablest if Gauss–Legendre points are used for the angles. The angular grid thus consists of points corresponding to a 9-point Gauss–Legendre quadrature ($\theta = 165.50^\circ, 146.72^\circ, 127.83^\circ, 108.92^\circ, 90^\circ, 71.08^\circ, 52.17^\circ, 33.28^\circ, \text{ and } 14.50^\circ$). In order to allow direct comparison with previous work,¹⁴ the two collinear configurations ($\theta=0$ and 180°) are also considered. The radial grid includes 15 points between 4.75 and $14a_0$. In this initial study the monomer HF distance is kept fixed at the experimental equilibrium value ($r_e = 1.73291a_0$) as in the work of O'Neil *et al.*¹⁴ All calculations were carried out with the GAUSSIAN 94 program suite.²⁰

For the weak interactions that exist in neutral Van der Waals complexes, it is essential to include the counterpoise correction.²¹ The need for this arises because, in a supermolecule calculation, each constituent can lower its energy artificially by taking advantage of basis functions of the other constituent, and the resulting stabilization is unphysical. The intermolecular energy $V(R, \theta)$ at each geometry is thus calculated as

$$V(R, \theta) \approx V^{\text{corr}}(R, \theta) = W_{\text{Ne-HF}}(R, \theta) - W_{\text{Ne}}(R, \theta) - W_{\text{HF}}(R, \theta), \quad (1)$$

where the quantities $W(R, \theta)$ are the electronic energies of the complex and the two monomers calculated in the complete supermolecule basis set.

A. Quality of the unmorphed results

In this section the unmorphed *ab initio* potentials are compared and discussed. Two-dimensional surfaces were calculated at the CCSD(T) level with the aug-cc-*p*VDZ, aug-cc-*p*VTZ, and ONeil basis sets. In addition, to provide error estimates, cuts at $\theta=0, 90^\circ$, and 180° were calculated with the aug-cc-*p*VQZ basis.

The pointwise potential at each value of R can easily be converted into an expansion in Legendre polynomials, $P_\lambda(\cos \theta)$,

$$V(R, \theta) = \sum_{\lambda=0}^8 V_\lambda(R) P_\lambda(\cos \theta). \quad (2)$$

The choice of Gauss–Legendre quadrature points as grid points avoids the (potentially unstable) matrix inversion needed to project out the radial strength functions $V_\lambda(R)$ from a regularly spaced angular grid. To define a complete potential surface, the radial strength functions are interpolated using the reproducing kernel Hilbert space scheme of Ho and Rabitz.¹³ This approach ensures smooth behavior of the interpolant and an exact reproduction of the initially calculated *ab initio* points. In addition, the procedure is readily extended to higher-dimensional problems.

Figure 1 shows the potentials obtained from different basis sets at $\theta=0, 90^\circ$, and 180° , and compares them with the “best” empirical potential described below. It may be seen that the diffuse basis functions are crucial to a good representation of the potential; at the CCSD(T) level, the aug-cc-*p*VDZ basis set gives only about two-thirds of the well depth, and even the aug-cc-*p*VTZ basis and aug-cc-*p*VQZ potentials are significantly too shallow.

At the linear Ne–HF geometry ($\theta=0$), CCSD(T) calculations using the ONeil basis set give a potential that is slightly shallower than for the aug-cc-*p*VTZ basis set. However, the CCSD(T) results are substantially deeper than those obtained from CEPA calculations using the same basis set by ONeil *et al.* themselves.¹⁴

The results and even the relative orderings are different at the T-shaped geometry. There, the CCSD(T) well depth for the ONeil basis set is quite similar to the VQZ result, although the intermolecular distance at the minimum is somewhat larger. The VTZ potential is much shallower at this geometry. Once again the CEPA results are considerably shallower than the CCSD(T) results with the same basis set.

The effects observed for the T-shaped geometry are repeated at the Ne–F–H configuration. The ONeil basis gives a slightly larger well depth than the VQZ basis, again at a slightly larger intermolecular distance. As will be seen below, the overall shape of the potential obtained with the ONeil basis set is significantly better than those from even the aug-cc-*p*VQZ basis set.

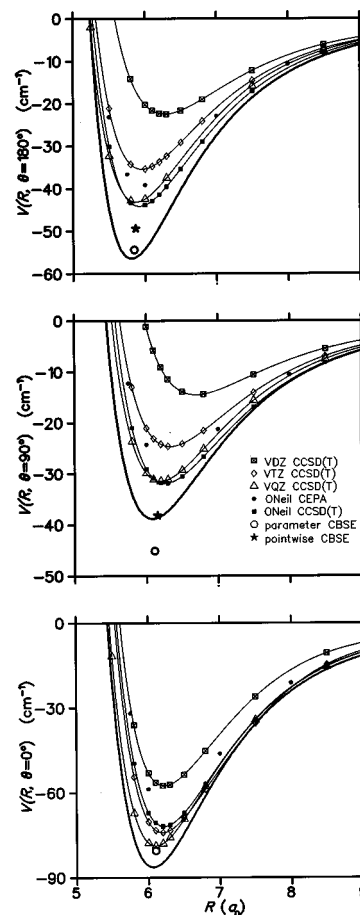


FIG. 1. Comparison of results using different basis sets and correlation treatments for Ne–HF. CCSD(T) calculations are shown as symbols joined by lines for basis sets aug-cc-*p*VDZ (open diamonds); aug-cc-*p*VTZ (open triangles); aug-cc-*p*VQZ (open circles); and ONeil *et al.* (filled squares). The results obtained by ONeil *et al.* using CEPA calculations with this basis set are also shown (filled circles). The isolated points below the *ab initio* curves show the results of complete basis set extrapolation (CBSE) using the “parameter” and “pointwise” methods described in the text. The solid line shows the empirical potential of Lovejoy and Nesbitt (Ref. 15).

B. Complete basis set extrapolation

One advantage of the correlation-consistent basis sets is that their systematic construction scheme makes it possible to carry out complete basis set extrapolation (CBSE).²² The quantity X to be extrapolated is taken to be a function of the basis set size n , where $n=2$ for aug-cc-*p*VDZ, $n=3$ for aug-cc-*p*VTZ, and so forth. The quantity $X(n)$ is fitted to an exponentially decaying function of n , and the extrapolation to $n=\infty$ gives predictions for arbitrarily large basis sets.

In the present case the extrapolation can be done in several different ways. One approach is to consider the well depth and equilibrium separation on each angular cut to be functions of the basis size n and to extrapolate them to $n=\infty$. This is referred to as “parameter” extrapolation here. Alternatively, the interaction energy can be extrapolated at each value of R to produce a potential curve, and the well depth and equilibrium separation extracted from this. This is called “pointwise” extrapolation here. We have tried both methods, and the results are included (where possible) in Fig. 1. We find that the two approaches give quite different re-

sults: extrapolating the well depths gives a potential that is systematically deeper than extrapolating the potential points themselves.

It is not always possible to carry out both pointwise and parameter extrapolations. For example, at the linear Ne–H–F configuration it is possible to extrapolate the well depths but the variation of R_e with n does not allow the extraction of a CBSE limit. The symbol indicating the parameter extrapolation corresponds to the CBSE of the well depth and the equilibrium separation on the aug-cc- p VQZ curve. The pointwise extrapolation is also impossible in this case: the pointwise extrapolated curve disappears towards $V = -\infty$ when the three potential curves are equally separated, which occurs just inside $R = 5.8a_0$.

Even the extrapolation of the potential points can be done in two different ways: the extrapolation can be done either for the “raw” supermolecule and monomer energies [$W(R, \theta)$ in Eq. (1)], or for the counterpoise-corrected interaction energy $V(R, \theta)$. Extrapolating $V(R, \theta)$ seems at first sight to be preferable, since the extrapolation is shorter and it is to be hoped that some of the basis-set errors will cancel. Indeed, van Mourik and Dunning have reported that extrapolating $W(R, \theta)$ does not converge regularly for Ar–HF.²³ Unfortunately, $V(R, \theta)$ is not strictly variational, so its convergence with basis set size may not be uniform; this is also seen in Fig. 1: at distances around $R = 7a_0$, the VQZ potential for $\theta = 0$ is actually *shallower* than the VTZ potential, and the extrapolation of $V(R, \theta)$ fails.

It is clear that CBSE must be applied with some care and circumspection for intermolecular forces, and that its results should be treated with caution.

IV. POTENTIAL AND COORDINATE SCALING

It is clear from the previous section that there is room to improve on the *ab initio* surfaces. Indeed, Lovejoy and Nesbitt¹⁵ have already used their experimental results on Ne–DF to adjust the CEPA surface of O’Neil *et al.*¹⁴ Their approach was to modify the well depth and minimum position for the $V_0(R)$ term in the potential to reproduce the binding energy and rotational constant of the ground state in Ne–FD ($v = 1$). Then $V_1(R)$ and $V_2(R)$ were scaled by constant factors to bring the Σ and Π bend frequencies into agreement. This procedure gave a potential which was able to give a satisfactory account of the experimental observables.¹⁵

The approach taken in the present work is more comprehensive. Imagine the potential energy surface to be carved in a block of rubber. The block can be stretched and bent in various directions and by different amounts to accommodate the experimental observables. This morphing procedure can be written mathematically as

$$V_{\text{morph}}(R, \theta) = v(R, \theta) V_{\text{orig}}(\rho(\theta) \cdot R, \theta). \quad (3)$$

The aim then, is to determine the functions $v(R, \theta)$ and $\rho(\theta)$ to give an optimal fit to the reference data (which are the infrared spectra in the present case). Since only interpolation and not fitting is involved in defining $V_{\text{orig}}(R, \theta)$, there are

no errors due to poor fitting of the *ab initio* points (though it is still necessary to ensure that there are enough points to define the shape properly).

The form of Eq. (3) needs some explanation. At first sight, it might be thought that an energy scaling $v(R, \theta)$ alone would be enough to achieve the changes required. However, such a representation is inefficient: there are points (or actually surfaces) at which $V_{\text{orig}}(R, \theta)$ is zero, and they are not the same as those at which $V_{\text{morph}}(R, \theta)$ is zero. To transform one into the other using just an energy scaling would thus require a scaling function $v(R, \theta)$ with poles and zeroes. Such a function is difficult to parametrize and to visualize. It is better to start by defining a distance scaling function $\rho(\theta)$ that maps the zeros of $V_{\text{orig}}(R, \theta)$ onto those of $V_{\text{morph}}(R, \theta)$, and *then* to define an energy scaling $v(R, \theta)$ to deal with the rest of the corrections needed. The energy scaling function can then be expected to be a smooth function of the coordinates.

The generalization of Eq. (3) to higher-dimensional problems is straightforward. The distance scaling function ρ needs to be a function of all coordinates *except* R , while the energy scaling function v is a function of all coordinates *including* R .

In the present work, we used the functional forms

$$\rho(\theta) = \sum_{\lambda} \rho_{\lambda} P_{\lambda}(\cos \theta),$$

$$v(R, \theta) = \sum_{\lambda k} v_{\lambda k} P_{\lambda}(\cos \theta) f_k(R). \quad (4)$$

In the present work, the sums were restricted to $\lambda_{\text{max}} = 2$ and $k_{\text{max}} = 0$, with $f_0(R) = 1$ (so that $v(R, \theta)$ is actually independent of R here). These restrictions could be relaxed if the experimental data were sufficient. The lengths of the expansions were chosen after considering the experimental data available, as described below. The morphing procedure is actually equivalent to a least-squares fit to determine the parameters v_{00} , v_{10} , v_{20} , ρ_0 , ρ_1 , and ρ_2 .

The actual morphing was done using the I-NOLLS program,²⁴ which is an interactive least-squares fitting package that gives the user detailed control over the progress of the fit, with the ability to inspect statistical information and to add or remove experimental data and fitting parameters as the fit proceeds.

V. COMPARING EXPERIMENT AND THEORY

The experimental results from the infrared spectra can be expressed in various ways, and the different representations are by no means equivalent for fitting purposes. The “raw” infrared observables are line positions for individual vibration–rotation lines. However, it is not desirable to fit to such line positions directly, because high-precision quantities such as rotational constants contain direct information about intermolecular distances which can be obscured in fitting to the line positions themselves. More specifically, we need to be able to fit the *spacings* between rotational levels with considerably greater precision than the vibrational frequencies.

This argument can be taken one stage further. Rotational level spacings are measured for $J=0$ to 1 and for $J=1$ to 2 (and, of course, for higher J values). The $J=0$ to 1 spacing is very close to $2B$ (where B is the rotational constant, very roughly 0.15 cm^{-1} for Ne–HF). The $J=1$ to 2 spacing is very close to $4B$, and is thus almost exactly twice the 0 to 1 splitting. The deviation from linear dependence of the two spacings is contained in the centrifugal distortion constant D , which is a tiny quantity (around 10^{-6} cm^{-1}) but nevertheless contains important information: for the Van der Waals ground state, D is closely related to the radial curvature of the potential around the minimum. It is unrealistic to expect a parametrized potential to reproduce the rotational spacings themselves to better than, say, 10^{-4} cm^{-1} , so to include the rotational spacings as they stand obscures the curvature information. Instead of $E_1 - E_0$ and $E_2 - E_1$ (where E_J is the energy for rotational quantum number J), it is much better to fit to $E_1 - E_0$ and the linear combination $\Delta = (-E_2 + 3E_1 - 2E_0)/24$; the latter quantity is approximately equal to D , and isolates the curvature information.

A similar argument applies for the l -type doubling splittings that may be obtained from the spectra of the (1110) \leftarrow (0000) bands. The P - and R -branch lines terminate on upper states of $\Pi(e)$ symmetry, and the Q -branch lines terminate on states of $\Pi(f)$ symmetry. The splitting between the e and f states of a given J depends on the extent of Coriolis mixing of the $\Pi(e)$ states with nearby Σ states. As before, it is better to represent this by the energy spacing between the $J=1$ e and f states than by the actual energies of these levels.

For each vibrational level, the quantities that are actually included in the fit are thus:

- the energy of the lowest rotational level, with $J=K$ (and f symmetry in the case of $K=1$), relative to the $J=0$ level of the (1000) state;
- the spacing between the lowest ($J=K$) and next lowest ($J=K+1$) rotational levels (again for f symmetry in the case of $K=1$);
- the second-order difference $-E_2 + 3E_1 - 2E_0$, which is approximately equal to $24D$ (included for the (1000) states only);
- the spacing between the $J=1(e)$ and $1(f)$ levels (for $K=1$ states only).

The experimental data available for Ne–HF and Ne–DF contain rather different information. For Ne–HF, the rotational constants for the (1000) and (1110) states may be viewed qualitatively as containing information on the position of the radial minimum for angles around $\theta=0^\circ$ and 90° , respectively, while the spacing between the two vibrational states depends upon the potential anisotropy. The Ne–HF spectra contain little information on the potential around $\theta=180^\circ$. By contrast, the Ne–DF Σ bend state (1100) has considerable amplitude around $\theta=180^\circ$, so the combination of the Ne–HF and Ne–DF spectra allows the potential to be determined reliably across the whole angular range. The Van der Waals stretch for Ne–DF also helps determine the radial curvature around the minimum, and hence the well depth; for

Ne–HF such information comes only from the centrifugal distortion constants, which are rather less reliable.

We have carried out close-coupling calculations of the bound vibration–rotation states for both Ne–HF and Ne–DF. These calculations make no dynamical approximations (except for the neglect of potential matrix elements off-diagonal in the monomer vibrational quantum number v). The total wave function is expanded in a space-fixed basis set made up of products of angular functions for the internal rotation of the HF monomer and the rotation of Ne and HF about one another. The resulting coupled equations are solved using the BOUND program,^{25,26} which is a general-purpose package for coupled-channel calculations on Van der Waals complexes. All basis functions for monomer rotational functions up to $j=8$ were included in the calculations. The reduced masses for Ne–HF and Ne–DF were taken to be $9.999\,665m_u$ and $10.244\,89m_u$, respectively. Since the experimental splittings refer to the $v=1$ vibrationally excited states of HF and DF, the rotational constants used were $b_{\text{HF}} = 19.787\,478\text{ cm}^{-1}$ and $b_{\text{DF}} = 10.564\,179\text{ cm}^{-1}$. The coupled equations were propagated from $R_{\text{min}} = 2.0\text{ \AA}$ to $R_{\text{max}} = 10.0\text{ \AA}$, extrapolating to zero step size from log-derivative interval sizes of 0.05 and 0.10 a_0 using Richardson h^4 extrapolation.

The center of mass of DF is shifted from that of HF. The intermolecular potential is defined in the coordinate system appropriate to Ne–HF, so that a coordinate transformation is needed when calling the potential routine for the Ne–DF species.²⁷ In reality, the potentials for Ne–HF and Ne–DF will also differ slightly because they correspond to different averages over the monomer stretching coordinate r , but this effect is neglected in the present work.

VI. MORPHED POTENTIALS

The parameters defining the morphing transformations for the three CCSD(T) potentials are summarized in Table I, together with some of the important features of the resulting potentials. The potentials themselves are shown as contour plots on the right-hand side of Fig. 2, with the unmodified *ab initio* potentials included on the left for comparison. The fits to the experimental results are reasonably good in all cases.

The results confirm that all the *ab initio* potentials are considerably too shallow; even the aug-cc- p VQZ potential needs to have its depth at $\theta=0^\circ$ increased by 10% to match the experimental results. This agrees with the conclusions of Lovejoy and Nesbitt.¹⁵ However, the really striking feature of Fig. 2 is that the three different morphed potentials are so similar. As discussed above, the original CCSD(T) potentials from the aug-cc- p VTZ and ONeil basis sets have substantially different angular behavior, but this has been dealt with by the morphing process and the final potentials are very similar. Even the potential based on the aug-cc- p VdZ basis set, which was originally too shallow by a factor of almost two, is quite reasonable after morphing (though the fit to the experimental data is not quite as good in this case).

The functional form to describe the morphing process was restricted to $\lambda \leq 2$ in Eq. (3). This is a reasonable choice, because there are data for three different vibrational states of Ne–DF, and thus three independent pieces of information

TABLE I. Parameters describing the morphing process in Eq. (3).

Level	CCSD(T)	CCSD(T)	CCSD(T)	MP2	CEPA ^a
Basis	aug-cc- <i>p</i> VDZ	aug-cc- <i>p</i> VTZ	ONeil ^a	ONeil	ONeil
v_{00}	2.332 113	1.453 165	1.207 692	1.762 227	1.360 635
v_{10}	-0.178 298	-0.157 551	0.039 967	0.056 955	0.041 684
v_{20}	-0.541 355	-0.156 824	-0.010 422	-0.200 212	-0.042 862
ρ_0	1.085 299	1.030 406	1.023 136	1.056 240	1.030 940
ρ_1	-0.029 569	-0.009 168	-0.001 128	-0.002 096	-0.002 729
ρ_2	-0.026 990	-0.012 074	-0.005 242	-0.014 480	-0.003 097
$\epsilon(0^\circ)$ (cm ⁻¹)	-93.08	-84.26	-88.90	-89.15	-88.50
$\epsilon(\text{TS})$ (cm ⁻¹)	-37.75	-37.69	-38.45	-38.47	-38.51
$\epsilon(180^\circ)$ (cm ⁻¹)	-44.24	-51.63	-51.11	-49.61	-49.96
$R_m(0^\circ)$ (Å)	3.197	3.248	3.235	3.223	3.227
$R_m(\text{TS})$ (Å)	3.227	3.233	3.229	3.226	3.233
$R_m(180^\circ)$ (Å)	3.055	3.069	3.075	3.070	3.062
$\theta(\text{TS})$	89°	94°	97°	94°	89°

^aReference 14.

about each of $v(\theta)$ and $\rho(\theta)$. The experimental results for Ne–HF improve the redundancy of the data set, but do not contain much independent information. To test the truncation, we also tried to determine morphing transformations with $\lambda_{\text{max}}=3$. The overall agreement between the calculated and observed spectroscopic observables did improve slightly, but the fit became much more correlated. The best single measure of correlation is the ratio of the largest and smallest singular values of the Jacobian matrix, and this quantity increased by a factor of 10 when terms with $\lambda=3$ were included. As a result, the correlated uncertainties in the fitted parameters also increased markedly. In our judgment, the fits with $\lambda_{\text{max}}=3$ are less reliable than those with $\lambda_{\text{max}}=2$, and they are not presented here.

A. What level of correlation treatment is necessary?

In view of the similarity of the morphed potentials from CCSD(T) calculations with different basis sets, it is tempting to ask just how primitive an *ab initio* potential can give satisfactory results after morphing.

It is fairly clear that a self-consistent field (SCF) potential, which would have almost no attractive well at some angles for Ne–HF, would not be adequate. Some kind of correlation treatment is essential. Methods such as Møller–Plesset (MP) perturbation theory are particularly attractive, because they are computationally inexpensive and are thus affordable for quite large systems. We have therefore calculated an MP2 potential for Ne–HF using the basis set of ONeil *et al.*,¹⁴ and applied the morphing procedure to it. Each point on this surface costs a factor of five less than a point on the corresponding CCSD(T) surface. The results are included in Table I and the resulting potential is shown in Fig. 3. It may be seen that the morphed potential is once again remarkably similar to the ones obtained from higher-level calculations. Although the spectroscopic observables are not as accurately reproduced ($\sigma^2=13.3$) as with the corresponding CCSD(T) potential, the agreement between theory and experiment is generally satisfactory.

B. The recommended Ne–HF potential

In the previous sections, we have developed four different morphed potentials for Ne–HF, all of which reproduce the experimental data reasonably well. It is legitimate to ask which of these is the “best” potential. One answer to this is given by the σ^2 value, which is the sum of squares of the (weighted) residuals (obs–calc values). These values are included in Table II, and it may be seen that the morphed potential based on CCSD(T) calculations on the ONeil basis set is rather better than the others, with a σ^2 value about half that for the best of the rest.

Another answer to the question is given by considering the optimized parameter values themselves. Since the principle of morphing is to change the *ab initio* potential as little as possible, we have most confidence in the morphing if the scalings v_{00} and ρ_0 are close to 1 and the corresponding anisotropies v_{10} , v_{20} , ρ_1 , ρ_2 , etc. are as small as possible. On this basis, the CCSD(T) potential calculated with the ONeil basis is clearly the best by far: v_{00} is about 1.2 [compared to 1.45 for the CCSD(T) potential calculated with the aug-cc-*p*VTZ basis set] and both v_{10} and v_{20} are less than 0.04 (compared to values around -0.15). CCSD(T) calculations on the ONeil basis set clearly give a potential with a reasonable depth and a very realistic anisotropy even before adjustment, and this provides an excellent starting point for morphing.

Although we have not calculated a full surface using the aug-cc-*p*VQZ basis set, it is clear from Fig. 1 that CCSD(T) calculations with this basis set do not give as good an angular shape as those using the ONeil basis set. They overemphasize the well at $\theta=0$ compared to those at $\theta=90^\circ$ and 180° .

The *ab initio* potential obtained from MP2 calculations on the ONeil basis set is also satisfactory after morphing, with a σ^2 value only 30% larger than the “best” potential. Nevertheless, the shape of the unaltered MP2 potential is definitely not as good as the CCSD(T) potential. The value of v_{20} for the MP2 potential in Table I is close to -0.2.

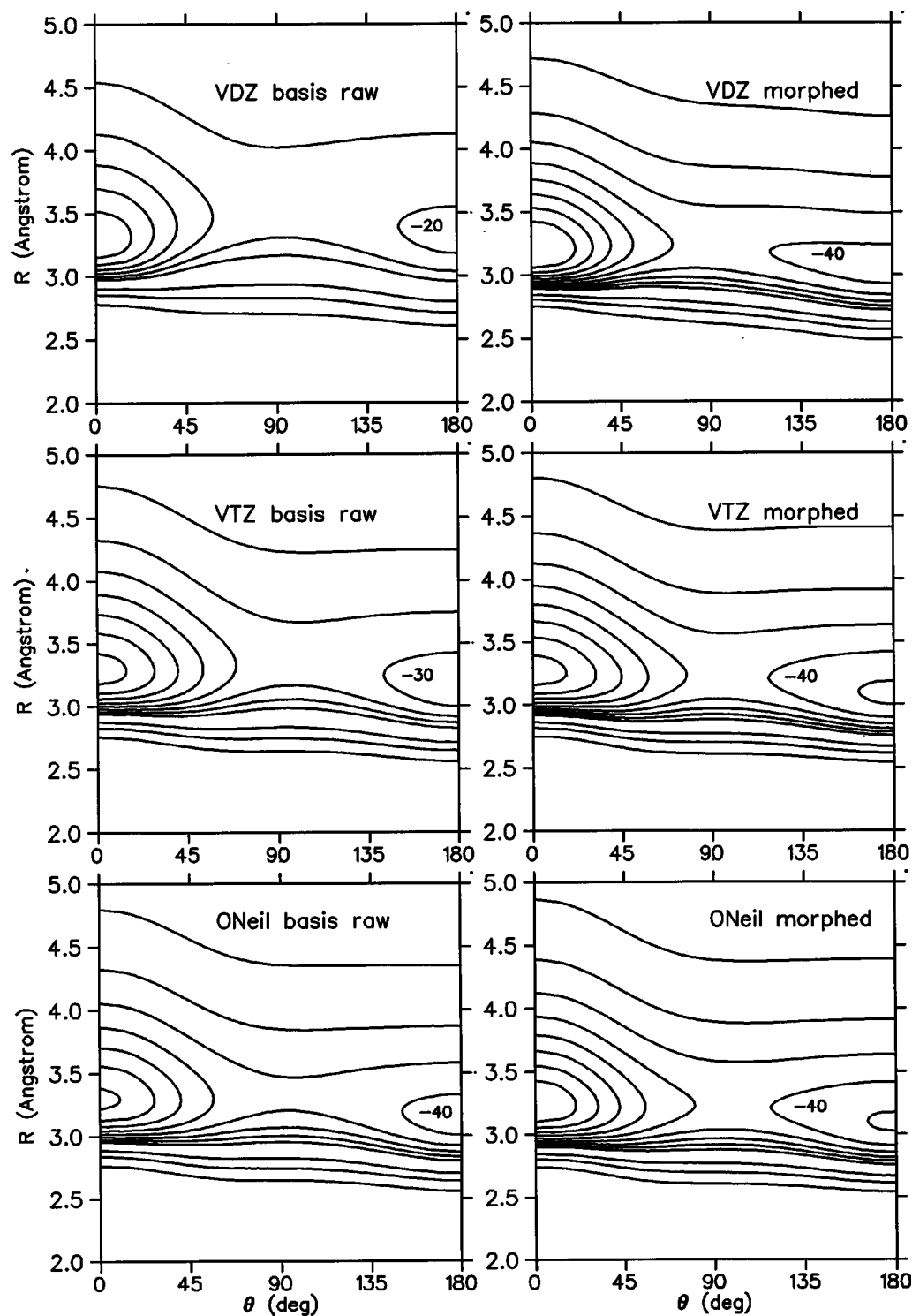


FIG. 2. Contour plots of the Ne-HF potential energy surfaces from CCSD(T) calculations with different basis sets, before and after morphing to reproduce the experimental results.

As described above, Lovejoy and Nesbitt¹⁵ have previously obtained a potential for Ne-DF by adjusting the CEPA potential of ONeil *et al.*¹⁴ They did not include the Ne-HF data, and the CEPA potential is considerably inferior to the CCSD(T) potential, so the present morphed CCSD(T) potential is to be preferred. Nevertheless, the adjusted potential of Lovejoy and Nesbitt is of quite good quality. We also investigated the effect that our morphing procedure has on the

original CEPA potential, and the results are included in Table I. The quality of fit is slightly poorer than for our “best” potential. Comparing the values of the scaling factors, it can be concluded that the CEPA potential is considerably superior to the MP2 potential but not quite as good as the CCSD(T) potential calculated here with the same basis set.

It must be remembered that the potentials obtained here

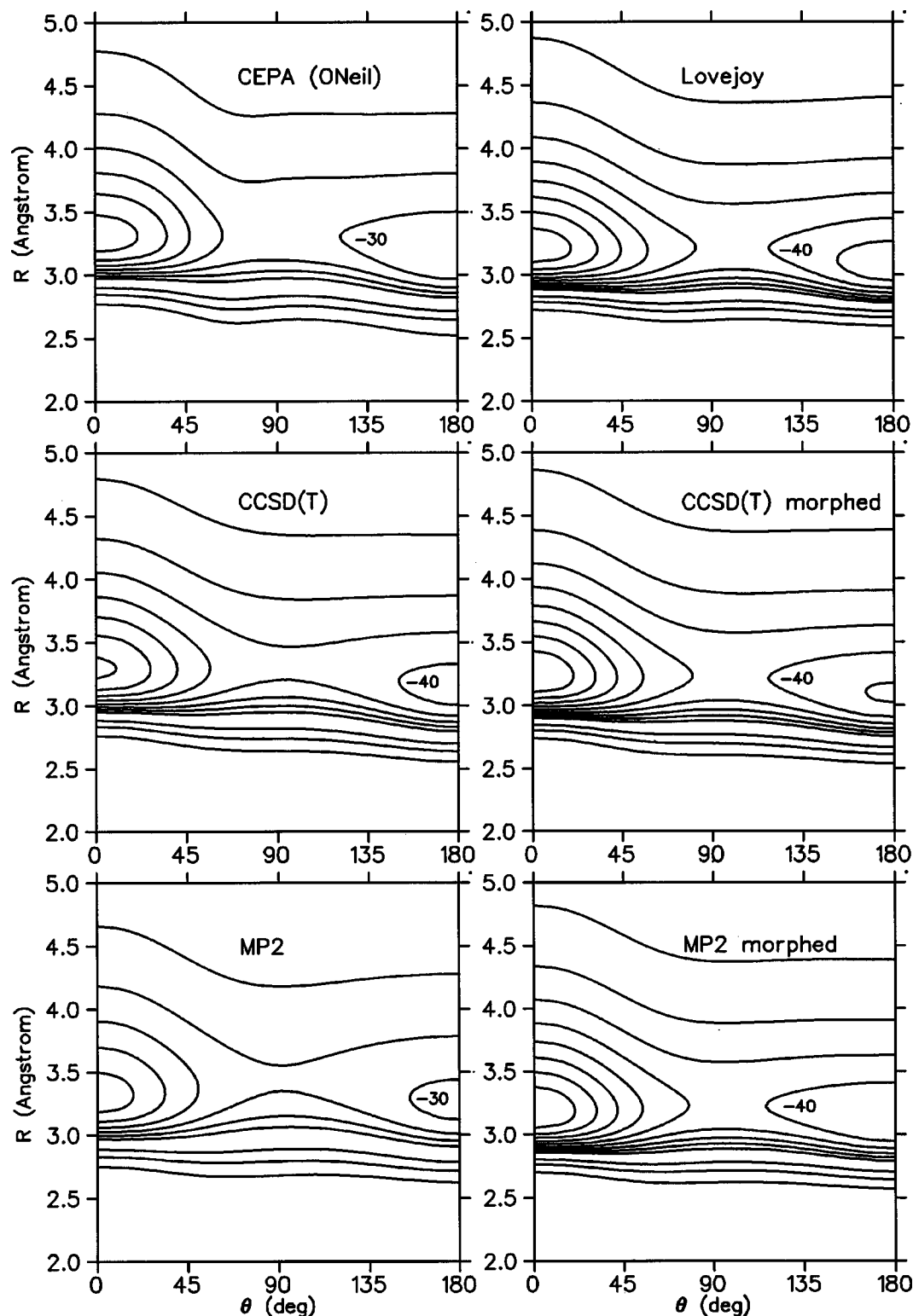


FIG. 3. Contour plots of the Ne–HF potential energy surface from MP2 calculations on the basis set of Ref. 14, before and after morphing to reproduce the experimental results. The potential is compared with the CEPA surface obtained using the same basis set (Ref. 14) and the adjusted potential of Lovejoy and Nesbitt (Ref. 15).

have been fitted primarily to data that refer to the $v = 1$ state of DF. For Ar–HF¹ and Ar–HCl,² it was possible to extract empirical potentials with an explicit dependence on the mass-reduced quantum number $\eta = (v + 1/2)/\sqrt{\mu_{\text{HX}}}$. The experimental data available for Ne–HF and Ne–DF are not

sufficient to do this reliably at present. Although the *ab initio* calculations in the present work were carried out for $r = r_e$, the *morphed* potentials should be interpreted as effective potentials, vibrationally averaged over the $v = 1$ state of DF. The effective potentials for other states of DF, or of HF, will

TABLE II. Comparison of spectroscopic observables for Ne–HF and Ne–DF from the literature and this work. All labels refer to the morphed PESs calculated with the CCSD(T) method except for the adjusted potential which relies on the CEPA work of Ref. 14.

	obs ^a	<i>p</i> VDZ basis	<i>p</i> VTZ basis	ONeil basis ^a	Uncertainties
Ne–HF					
ground state (1000)					
binding energy $D_0(v=1)$ (cm ⁻¹)		-31.131	-32.963	-32.830	
$E_{J=1} - E_{J=0}$ (cm ⁻¹)	0.2989	0.3002	0.2996	0.2997	0.0002
$\Delta(10^{-6}$ cm ⁻¹)	19.70	19.60	19.59	19.54	0.17
Π bend (1110)					
$E_{J=1f} - E_{J=0}(1000)$ (cm ⁻¹)	44.0340	43.9817	44.1135	44.0716	0.01
$E_{J=2f} - E_{J=1f}$ (cm ⁻¹)	0.5938	0.5930	0.5936	0.5936	0.0004
$E_{J=1e} - E_{J=1f}$ (10 ⁻³ cm ⁻¹)	20.5800	20.3710	19.5638	19.4762	0.2
Ne–DF					
ground state (1000)					
binding energy $D_0(v=1)$ (cm ⁻¹)	-35.1 ± 0.76	-33.424	-35.111	-35.009	
$E_{J=1} - E_{J=0}$ (cm ⁻¹)	0.2961	0.2968	0.2956	0.2959	0.0002
$\Delta(10^{-6}$ cm ⁻¹)	16.08	16.24	16.66	16.60	0.17
Σ bend (1100)					
$E_{J=0} - E_{J=0}(1000)$ (cm ⁻¹)	19.5295	19.5413	19.5378	19.5380	0.01
$E_{J=1} - E_{J=0}$ (cm ⁻¹)	0.2689	0.2690	0.2689	0.2689	0.0002
Σ stretch (1001)					
$E_{J=0} - E_{J=0}(1000)$ (cm ⁻¹)	23.3811	23.3729	23.3816	23.3809	0.01
$E_{J=1} - E_{J=0}$ (cm ⁻¹)	0.2382	0.2362	0.2384	0.2377	0.0002
Π bend (1110)					
$E_{J=1f} - E_{J=0}(1000)$ (cm ⁻¹)	27.2791	27.3208	27.2222	27.2533	0.01
$E_{J=2f} - E_{J=1f}$ (cm ⁻¹)	0.5830	0.5817	0.5826	0.5823	0.0004
$E_{J=1e} - E_{J=1f}$ (10 ⁻³ cm ⁻¹)	22.9800	23.4449	23.1993	23.2908	0.2
weighted σ^2	...	27.9	19.6	10.2	...

^aReference 14.

be slightly different; indeed, the relatively poor fit to the rotational constants of Ne–HF can largely be attributed to this effect.

VII. CONCLUSIONS

We have described a method for morphing an *ab initio* potential energy surface to match experimental data. We introduce both a coordinate scaling and an energy scaling, and allow both scalings to be (slow) functions of the coordinates. We have tested the method on Ne–HF, and determined scaling functions by fitting to the high-resolution infrared spectra of Nesbitt *et al.*¹⁶ for Ne–HF and Lovejoy and Nesbitt¹⁵ for Ne–DF. The resulting potential energy surfaces are remarkably insensitive to the quality of the *ab initio* surface used as a starting point. Even MP2 calculations using the basis set described by ONeil and co-workers¹⁴ give reasonable results after morphing. The method provides a workable approach for applying to quite large systems.

ACKNOWLEDGMENTS

M.M. acknowledges financial support from the Schweizerischer Nationalfonds zur Förderung der wissenschaftlichen Forschung. The calculations were carried out on a Silicon Graphics Origin 2000 computer system, which was pur-

chased with funding from the Engineering and Physical Sciences Research Council. We are grateful to Dr. Lydia Heck for computational assistance.

¹J. M. Hutson, J. Chem. Phys. **96**, 6752 (1992).

²J. M. Hutson, J. Phys. Chem. **96**, 4237 (1992).

³R. J. Le Roy, C. Bissonette, T. H. Wu, A. K. Dham, and W. J. Meath, Faraday Discuss. **97**, 81 (1994).

⁴J. M. Hutson, A. Ernesti, M. M. Law, C. F. Roche, and R. J. Wheatley, J. Chem. Phys. **105**, 9130 (1996).

⁵M. Quack and M. Suhm, J. Chem. Phys. **95**, 28 (1991).

⁶M. J. Elrod and R. J. Saykally, J. Chem. Phys. **103**, 933 (1995).

⁷F. B. Brown and D. G. Truhlar, Chem. Phys. Lett. **117**, 307 (1985).

⁸G. Jansen, J. Chem. Phys. **105**, 89 (1996).

⁹K. Higgins, F.-M. Tao, and W. Klemperer, J. Chem. Phys. **109**, 3048 (1998).

¹⁰J. M. Bowman and B. Gazdy, J. Chem. Phys. **94**, 816 (1991).

¹¹B. Gazdy and J. M. Bowman, J. Chem. Phys. **95**, 6309 (1991).

¹²J. M. Bowman and B. Gazdy, Chem. Phys. Lett. **200**, 311 (1992).

¹³T. S. Ho and H. Rabitz, J. Chem. Phys. **104**, 2584 (1996).

¹⁴S. V. ONeil, D. J. Nesbitt, P. Rosmus, H.-J. Werner, and D. C. Clary, J. Chem. Phys. **91**, 711 (1989).

¹⁵C. M. Lovejoy and D. J. Nesbitt, J. Chem. Phys. **94**, 208 (1991).

¹⁶D. Nesbitt, C. M. Lovejoy, T. G. Lindeman, S. V. ONeil, and D. C. Clary, J. Chem. Phys. **91**, 722 (1989).

¹⁷G. T. Fraser and R. D. Suenram, J. Mol. Spectrosc. **140**, 141 (1990).

¹⁸T. H. Dunning, Jr., J. Chem. Phys. **90**, 1007 (1989).

¹⁹R. A. Kendall, J. T. H. Dunning, and R. J. Harrison, J. Chem. Phys. **96**, 6796 (1992).

²⁰GAUSSIAN 94, Revision E.2, M. J. Frisch, G. W. Trucks, H. B. Schlegel, P.

- M. W. Gill, B. G. Johnson, M. A. Robb, J. R. Cheeseman, T. Keith, G. A. Petersson, J. A. Montgomery, K. Raghavachari, M. A. Al-Laham, V. G. Zakrzewski, J. V. Ortiz, J. B. Foresman, J. Cioslowski, B. B. Stefanov, A. Nanayakkara, M. Challacombe, C. Y. Peng, P. Y. Ayala, W. Chen, M. W. Wong, J. L. Andres, E. S. Replogle, R. Gomperts, R. L. Martin, D. J. Fox, J. S. Binkley, D. J. Defrees, J. Baker, J. P. Stewart, M. Head-Gordon, C. Gonzalez, and J. A. Pople, GAUSSIAN, Inc., Pittsburgh, PA, 1995.
- ²¹S. F. Boys and F. Bernardi, *Mol. Phys.* **19**, 553 (1970).
- ²²D. E. Woon and T. H. Dunning, Jr., *J. Chem. Phys.* **99**, 1914 (1993).
- ²³T. van Mourik and T. H. Dunning, *J. Chem. Phys.* **107**, 2451 (1997).
- ²⁴M. M. Law and J. M. Hutson, *Comput. Phys. Commun.* **102**, 252 (1997).
- ²⁵BOUND computer program, Version 5, J. M. Hutson, distributed by Collaborative Computational Project No. 6 of the UK Engineering and Physical Sciences Research Council, 1993.
- ²⁶J. M. Hutson, *Comput. Phys. Commun.* **84**, 1 (1994).
- ²⁷H. Kreek and R. J. Le Roy, *J. Chem. Phys.* **63**, 338 (1975).